Effects of Hyperglycemia and Effects of Ketosis on Cerebral Perfusion, Cerebral Water Distribution, and Cerebral Metabolism

Nicole Glaser,[1] Catherine Ngo,[2] Steven Anderson,[2] Natalie Yuen,[2] Alexandra Trifu,[2] and Martha O'Donnell[2]

Diabetic ketoacidosis (DKA) may cause brain injuries in children. The mechanisms responsible are difficult to elucidate because DKA involves multiple metabolic derangements. We aimed to determine the independent effects of hyperglycemia and ketosis on cerebral metabolism, blood flow, and water distribution. We used magnetic resonance spectroscopy to measure ratios of cerebral metabolites (ATP to inorganic phosphate [Pi], phosphocreatine [PCr] to Pi, N-acetyl aspartate [NAA] to creatine [Cr], and lactate to Cr) and diffusion-weighted imaging and perfusion-weighted imaging to assess cerebral water distribution (apparent diffusion coefficient [ADC] values) and cerebral blood flow (CBF) in three groups of juvenile rats (hyperglycemic, ketotic, and normal control). ATP-to-Pi ratio was reduced in both hyperglycemic and ketotic rats in comparison with controls. PCr-to-Pi ratio was reduced in the ketotic group, and there was a trend toward reduction in the hyperglycemic group. No significant differences were observed in NAA-to-Cr or lactate-to-Cr ratio. Cortical ADC was reduced in both groups (indicating brain cell swelling). Cortical CBF was also reduced in both groups. We conclude that both hyperglycemia and ketosis independently cause reductions in cerebral high-energy phosphates, CBF, and cortical ADC values. These effects may play a role in the pathophysiology of DKA-related brain injury. *Diabetes* 61:1831–1837, 2012

C erebral injury caused by diabetic ketoacidosis (DKA) is an important complication of type 1 diabetes in children. Approximately 1% of children with DKA develop severe, life-threatening cerebral edema and cerebral injury (1). Many more children with DKA, however, develop subtle cerebral edema, which can be demonstrated using magnetic resonance diffusion-weighted imaging (2). Magnetic resonance spectroscopy (MRS) studies in these children show metabolic changes consistent with cerebral injury (3). Recent data also suggest that memory deficits are common in children with diabetes who have experienced DKA, suggesting that subtle cerebral injury may occur frequently (4).

Despite the growing evidence that DKA frequently results in subtle brain injuries in children, relatively little is understood about the pathophysiology of brain injury in this setting. Interestingly, magnetic resonance data from animal and human studies demonstrate that DKA is associated with initial cytotoxic cerebral edema, progressing to vasogenic edema during treatment with insulin and saline (2,5,6). In addition, DKA has been shown to be associated with diminished cerebral blood flow (CBF) in animal models (5,6). These findings are similar to those observed in hypoxic/ischemic brain injury. Although some decline in CBF likely results from hypocapnia and circulatory volume depletion during DKA, it is not clear that these disturbances alone are sufficient to cause cerebral injury. Whether other aspects of DKA contribute to cerebral injury by augmenting the reduction in CBF or by compromising cerebral metabolism in other ways is therefore important to investigate. In the current study, we aimed to determine the effects of hypoinsulinemic hyperglycemia and hypoinsulinemic ketosis on CBF, cerebral water distribution, and cerebral metabolism. We hypothesized that effects of one or both of these conditions might alter CBF and/or cerebral metabolism. If our hypothesis is correct, one or both of these conditions might predispose the brain to injury when other conditions (such as severe hypocapnia and/or circulatory volume depletion) are superimposed.

RESEARCH DESIGN AND METHODS

Hyperglycemia model. Juvenile rats (4–6 weeks of age) were administered an intraperitoneal injection of streptozotocin (100 mg/kg for rats <100 g; 130 mg/kg for rats >100 g). Rats were given unlimited access to water with 10% dextrose (D10 W; Fisher Scientific, Santa Clara, CA) in the first 24-h period after streptozotocin injection to prevent hypoglycemia and were subsequently allowed unlimited access to tap water and standard rat chow. Twenty-four hours after streptozotocin injection, rats were treated with subcutaneous insulin (Novolin 70/30 insulin: 3 units daily for rats <100 g, 4 units daily for rats 100–200 g, and 5 units daily for rats >200 g) for a period of 5 days to allow for resolution of any nonpancreatic toxicities of streptozotocin. Urine glucose and ketoacids (acetoacetate) were measured daily using Multistix urinalysis strips (Bayer, Santa Clara, CA) up to and including the day of imaging. Animals developing abnormal urine acetoacetate concentrations (above "trace" levels on urinalysis strips: 0.5 mmol/L) at any time prior to imaging were not used for the hyperglycemia model. Serum insulin concentrations were measured by radioimmunoassay (Millipore Rat Insulin RIA; Millipore, Billerica, MA). One day prior to magnetic resonance studies, rats received no insulin treatment and drinking water was changed to D10 W to promote hyperglycemia. Both this protocol and the protocol for the ketosis model (see below) were conducted in accordance with the Animal Use and Care Guidelines issued by the National Institutes of Health using protocols approved by the animal use and care committee at the University of California, Davis.

Ketosis model. As in the hyperglycemia model, juvenile rats (4–6 weeks) were used for this protocol. Rats were given a diet consisting of 50% standard rat chow (LabDiet 5001; Commercial Chow, Richmond, IN) and 50% high-fat diet (category no. D12492, OpenSource Diets, 60% fat; Research Diets) for a period of 5 days. For an additional 5 days, rats consumed only the high-fat diet. Twelve hours prior to imaging, rats were fasted and allowed access only to tap water. Using this protocol, we were able to reliably generate ketosis (β-hydroxybutyrate [βOHB] concentration >1.0 mmol/L, measured using Precision Xtra blood ketone test [Abbott Laboratories, Abbott Park, IL]). Rats that failed to develop the previously specified level of ketosis were not used in the study.

Diffusion-weighted imaging and perfusion-weighted imaging procedures.
Rats in both groups were anesthetized using Na pentobarbital (65 mg/kg i.p.), and then the left femoral vein and artery were cannulated with PE-50 polyethylene tubing as previously described (7). The femoral vein cannula was used for additional anesthesia as needed. The femoral artery cannula was used for blood sampling. A heating pad with circulating water (Gaymar, Orchard Park, NY) was used to maintain body temperature at 36.8–37.0°C throughout surgery and magnetic resonance studies. Rats were also subjected to tracheal intubation and ventilated (Harvard Small Animal Ventilator, Holliston, MA) throughout surgery and magnetic resonance studies. Ventilation was done to offset the tendency toward respiratory depression in the anesthetized rats and to insure similarity to previous studies of rats with DKA conducted by our group. Blood samples were taken for analysis of Pco_2 and pH immediately after intubation and the respiratory rate and tidal volume adjusted to maintain the Pco_2 level within the normal range. Magnetic resonance diffusion-weighted spin echo images were acquired using a 7-Tesla Bruker Biospec MRS/magnetic resonance imaging (MRI) system as previously described (7). apparent diffusion coefficient (ADC) values (10^{-6} cm^2/s) were determined from 6×4 pixel regions of interest for eight brain regions (six cortex and two striatum) using Paravision 4.0 software with four gradient strengths of 5–95 mT/m. In each rat, CBF (milliliters per 100 grams per second) was also determined, using perfusion-weighted imaging analysis with continuous arterial spin labeling (ASL) and a standard Bruker PERFPACK2 protocol (Bruker, Billerica, MA). ASL data were acquired using the same field of view and slice thickness as used for diffusion-weighted spin echo images, and the ASL regions of interest were chosen from the 128×128 matrix so as to measure CBF and ADC on the same voxels (7,8). Images from perfusion-weighted imaging were acquired in 4.37 min using echo time (TE)/repetition time (TR) 12.77 ms/1,023 ms with a 1-s Adiabatic-Fast-Passage labeling pulse in the presence of a 10 mT/m gradient to obtain inversion $\pm8,515$ Hz (±2 cm) from the isocenter (also slice center) for control and labeled images, respectively. T1 maps for the same voxels were also acquired from selected rats in each treatment group to correct CBF measurements for possible location- and treatment-dependent variations in T1.
MRS procedures. MRS measurements were performed in anesthetized rats in a horizontal bore magnet (Oxford Instruments, Oxford, U.K.) using a two-channel Biospec system (Bruker Biospin, Billerica, MA) running ParaVision software. A double-tuned ^{1}H/X Litz coil (Doty Scientific, Columbia, SC) was used, where X is tunable for 23 Na or ^{31}P. Field homogeneity was optimized by localized shimming on ^{1}H over a $9 \times 9 \times 9$ mm voxel of interest (VOI). The VOI was positioned inside the brain and selected to encompass as much of the cortex as possible. After shimming, ^{31}P and ^{1}H MRS data were acquired.
^{31}P MRS. An $8 \times 8 \times 8$ mm VOI was centered on the shimmed volume. Spectra were acquired in 43.2-min intervals using Bruker software for image-selected in vivo spectroscopy (TR = 4 s, 80 signals averaged, 25-Hz line broadening). Intracellular pH was calculated from the chemical shift of the inorganic phosphate (Pi) peak relative to the phosphocreatine (PCr) peak, using the equation intracellular pH = $6.7 + \log[(\text{shift} - 3.186)/(5.691 - \text{shift})]$ (9). PCr, β-ATP, and Pi peaks were integrated using NUTS software (Acorn NMR, Livermore, CA) and presented as ratios (ATP to Pi and PCr to Pi).
^{1}H MRS. A $7 \times 7 \times 7$ mm VOI was centered on the shimmed volume. Spectra were acquired in 2.8-min intervals using Bruker software for point-resolved spectroscopy (TR = 6,974 ms, 20 signals averaged, 2-Hz line broadening) with chemical-shift–selective pulses and dephasing gradients to suppress water. Cerebral ^{1}H metabolite peaks were identified according to their chemical shifts (10): N-acetylaspartate (NAA) (2.02 ppm), creatine (Cr) and PCr (3.0 ppm), lactate (1.38 ppm), and βOHB (1.15 ppm). With a TE of 132 ms, the lipid peak was suppressed, and the lactate and βOHB appeared as inverted peaks. The

NAA, Cr, lactate, and βOHB peaks were integrated using NUTS software and presented as ratios (NAA to Cr, lactate to Cr, and βOHB to Cr).
Statistical analyses. Differences in MRI and MRS measures and differences in insulin levels among the three groups (hyperglycemia, ketosis, and control) were evaluated using ANOVA with Scheffe test used post hoc to detect differences between specific pairs of groups. Differences in MRI measures among rats that did and did not have evidence of mild nephrotoxicity from streptozotocin injection were evaluated using the Wilcoxon rank-sum test. All statistical analyses were conducted using Stata SE 11.1 (StataCorp, College Station, TX). P values <0.05 were considered to represent statistical significance, and P values ≤0.10 were considered to represent a trend.

RESULTS

Hyperglycemia and ketosis models. Using the procedures described, substantial hyperglycemia was generated in the hyperglycemic rat model, with mean blood glucose concentrations of ~28 mmol/L (Tables 1 and 2). Daily urine ketone testing after administration of streptozotocin confirmed absence of ketosis in the hyperglycemic group. Of note, some rats in the hyperglycemic group had slightly decreased serum bicarbonate concentrations consistent with mild renal tubular acidosis (4 of 16 total rats used in the hyperglycemia studies; serum bicarbonate concentration range 16–19 mmol/L). This effect was attributed to renal toxicity of streptozotocin (11). Comparison of magnetic resonance measures in hyperglycemic rats with and without mild renal tubular acidosis (RTA), however, revealed no significant effect of mild RTA on the measures of interest (data not shown); therefore, results from all hyperglycemic rats were included in the data reported.

In the ketotic group, blood ketone concentrations achieved were within a range consistent with moderate ketosis in children with diabetes (Tables 1 and 2). Ketotic rats had normal blood pH and Pco_2 (factors that could independently affect CBF). Serum insulin concentrations in both the hyperglycemic group (0.13 ± 0.11 ng/mL, $n = 6$) and the ketotic group (1.16 ± 0.44 ng/mL, $n = 6$) were significantly lower than in the control group (2.52 ± 1.13 ng/mL, $n = 11$; $P < 0.01$ for hyperglycemia vs. control, $P = 0.015$ for ketosis vs. control, $P = 0.12$ for hyperglycemia vs. ketosis).
Cerebral blood flow. In both the hyperglycemic group and the ketotic group, there were significant reductions in CBF in the cerebral cortex in comparison with the control group (Fig. 1A). In the striatum, there was a trend toward reduction in CBF in both groups in comparison with controls, but these differences were just short of statistical significance.
Cerebral water distribution. Using diffusion-weighted imaging, we observed a significant reduction in ADC in

TABLE 1
Biochemical values in hyperglycemic and ketotic rats versus control rats used for diffusion-weighted and perfusion-weighted imaging studies

	Hyperglycemia	Ketosis	Control	P
n	9	10		—
Glucose (mmol/L)	30.0 (7.8)	6.1 (1.2)	7.9 (1.9)	<0.001 hyperglycemia vs. control, 0.71 ketosis vs. control
βOHB (mmol/L)	—	2.1 (0.9)	—	—
pH	7.37 (0.07)	7.38 (0.04)	7.42 (0.05)	0.08 hyperglycemia vs. control, 0.19 ketosis vs. control
Pco_2 (mmHg)	36 (7)	37 (4)	38 (6)	0.58 hyperglycemia vs. control, 0.97 ketosis vs. control
Serum sodium (mmol/L)	142 (6)	140 (4)	141 (4)	0.76 hyperglycemia vs. control, 0.98 ketosis vs. control
Serum chloride (mmol/L)	109 (7)	107 (3)	107 (4)	0.53 hyperglycemia vs. control, 1.0 ketosis vs. control
Serum bicarbonate (mmol/L)	21 (3)	24 (2)	27 (3)	<0.01 hyperglycemia vs. control, 0.12 ketosis vs. control

Data are means (SD) unless otherwise indicated.

TABLE 2
Biochemical values in hyperglycemic and ketotic rats versus control rats used for MRS studies

	Hyperglycemia	Ketosis	Control	P
n	7	7	7	—
Glucose (mmol/L)	26.6 (7.4)	6.6 (1.1)	7.8 (1.5)	<0.001 hyperglycemia vs. control, < 0.001 ketosis vs. control
βOHB (mmol/L)	—	2.0 (0.6)	—	—
pH	7.36 (0.08)	7.39 (0.06)	7.42 (0.06)	0.25 hyperglycemia vs. control, 0.65 ketosis vs. control
P_{CO_2} (mmHg)	41 (4)	39 (6)	41 (5)	0.95 hyperglycemia vs. control, 0.89 ketosis vs. control
Serum sodium (mmol/L)	142 (6)	142 (2)	139 (4)	0.45 hyperglycemia vs. control, 0.61 ketosis vs. control
Serum chloride (mmol/L)	108 (7)	107 (2)	106 (4)	0.78 hyperglycemia vs. control, 0.91 ketosis vs. control
Serum bicarbonate (mmol/L)	24 (3)	24 (2)	27 (3)	0.17 hyperglycemia vs. control, 0.17 ketosis vs. control

Data are means (SD) unless otherwise indicated.

the cerebral cortex, indicating cytotoxic cerebral edema, in both the hyperglycemic group and the ketotic group in comparison with the control group (Fig. 1B). In the striatum, the differences in ADC in comparison with control values were significant only in the hyperglycemic group.

Cerebral metabolism. Using phosphorus MRS, we detected significant reductions in brain ratios of PCr to Pi in the ketotic group and a trend toward reduction in the hyperglycemic group in comparison with controls (Fig. 2). Reductions in brain ATP-to-Pi ratios were significant in both the hyperglycemic group and the ketotic group in comparison with controls. Brain intracellular pH was not significantly different among the three groups. Using proton MRS, we did not detect any significant differences among the groups in brain ratios of NAA to Cr or any differences in brain lactate levels.

DISCUSSION

Cerebral injury caused by DKA shares several common features with hypoxic-ischemic brain injury. Early descriptions of postmortem findings in children who died of DKA-related brain injury showed features suggestive of ischemia (12,13). More recent studies demonstrate that DKA results in cytotoxic cerebral edema (cell swelling) progressing to vasogenic cerebral edema (increased extracellular fluid) during treatment with insulin and saline, a pattern similar to that observed in ischemia-reperfusion injury (2,7). Furthermore, brain NAA-to-Cr ratios are diminished in DKA and levels of high-energy phosphates are reduced, similar to findings in hypoxic-ischemic brain injury (5,14,15).

We have previously demonstrated that CBF is reduced in DKA, but the cause of this reduction is not fully understood (6). Cerebral vasoconstriction induced by hypocapnia and intravascular volume depletion may account for some reduction in CBF, but the degree of cerebral injury that occurs in at least some children is greater than might be expected to result from these conditions alone. It is possible that other conditions present during DKA might contribute to reducing CBF. In addition, the decrease in CBF observed during DKA is modest in comparison with that typically observed in stroke or other hypoxic-ischemic conditions, raising the question of whether some other aspect of DKA might augment the severity of injury caused by moderate CBF reductions. In the current study, we demonstrate that both hyperglycemia and ketosis are associated with reductions in cortical CBF. In addition, both conditions were associated with reduced brain levels of high-energy phosphates and reduced ADC values that could result from disturbances in membrane ion homeostatic mechanisms. These data suggest that hyperglycemia and/or ketosis may increase the vulnerability of the brain to injury.

Substantial data from previous studies in both humans and animal models demonstrate an association between hyperglycemia and worsening of hypoxic-ischemic brain injury (16–20). In animal studies of stroke, hyperglycemia is associated with increases in infarct volume, edema formation, neutrophil deposition in ischemic tissue, and lactate accumulation (19,21–23). Hyperglycemia is associated with impaired vascular endothelial function resulting in decreased vasodilation (24), as well as with decreased erythrocyte deformability and alterations in blood flow properties that might contribute to ischemia (25,26). Reduced CBF during hyperglycemia has also previously been reported in rats (27). Several studies suggest an association between hyperglycemia and increased morbidity and mortality from ischemic stroke (28–30), and some studies suggest that hyperglycemia may directly cause neuronal injury. In rats, hyperglycemia (streptozotocin-induced diabetes) has been found to result in alterations in neuronal structure and impaired memory (31,32).

The effects of ketosis in the setting of brain injury have been studied less extensively than the effects of hyperglycemia. In one study, acetoacetate was found to increase production of the vasoconstrictor endothelin-1 in brain microvascular endothelial cells (33). In addition, elevated concentrations of acetoacetate have been found to increase erythrocyte viscosity (34). In apparent contrast to these findings, however, some studies in rodents suggest a neuroprotective effect of ketosis in the setting of hypoxic-ischemic injury or traumatic injury (35–37). The mechanism for this apparent protective effect has been proposed to be related to diminished glycolytically-derived lactate production as well as decreased free radical generation (36). Conversely, studies of long-term effects of ketogenic diets suggest possible detrimental effects on memory and other cognitive functions in both rats and humans (38,39). Thus, the effects of ketosis are unclear and may vary in different physiologic settings. Our results demonstrate that ketosis (induced by a ketogenic diet) reduces CBF and decreases brain levels of high-energy phosphates, which would appear to suggest adverse consequences. In apparent contrast, a study of ketone infusion in adult rats found an increase in CBF—a finding one might not predict from our results (40). The reason for the variation in results between those data and our data is unclear. The ketone infusion model induces metabolic alkalosis, and it is possible that alterations in acid-base balance may have affected CBF. Differences in insulin
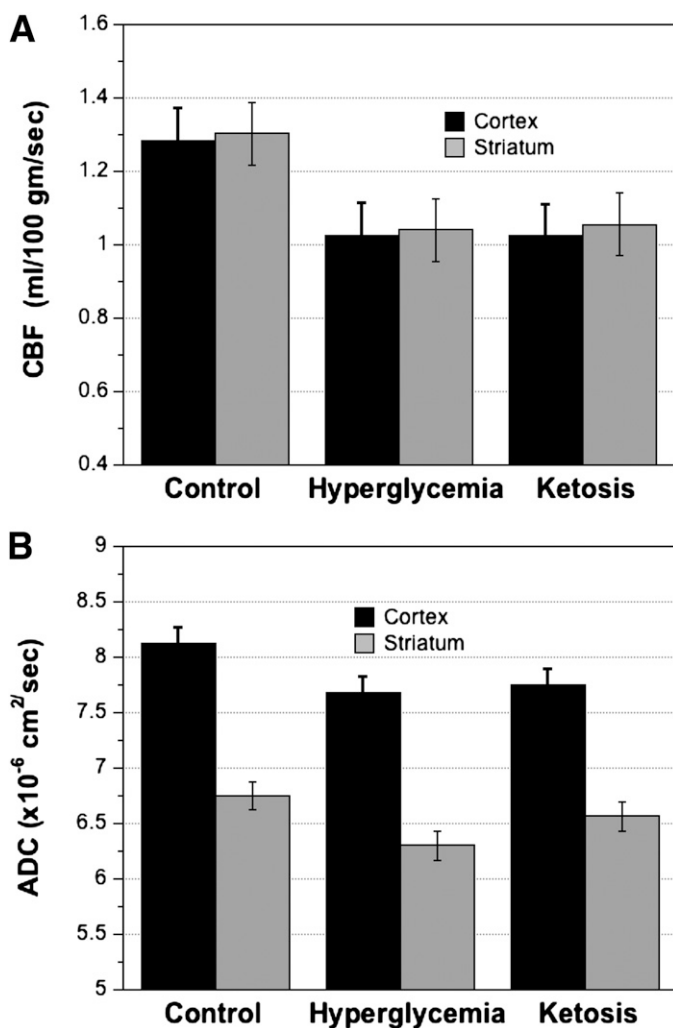
FIG. 1. *A*: CBF in hyperglycemic and ketotic rats in comparison with control rats measured using arterial spin labeling (means ± SE for 10 ketotic, 10 control, and 9 hyperglycemic rats). Cortex: $P = 0.03$ hyperglycemic vs. control, $P = 0.02$ ketotic vs. control. Striatum: $P = 0.06$ hyperglycemic vs. control, $P = 0.07$ ketotic vs. control. *B*: Apparent diffusion coefficients in hyperglycemic rats and ketotic rats in comparison with control rats (means ± SE for 10 ketotic and 10 control rats and 9 hyperglycemic rats). Cortex: $P = 0.004$ hyperglycemic vs. control, $P = 0.012$ ketotic vs. control. Striatum: $P = 0.019$ hyperglycemic vs. control, $P = 0.46$ ketotic vs. control.

concentrations between the two models might be another possible explanation for the variation in results (see below).

Our data suggest that both hyperglycemia and ketosis result in similar alterations in CBF, cerebral water distribution, and cerebral metabolism. Although these states are dissimilar from a metabolic standpoint, both conditions are associated with low serum insulin concentrations, raising the intriguing possibility that the findings may be related to insulin deficiency rather than direct effects of hyperglycemia or ketosis. Although the role of insulin in the brain was previously thought to be minimal, data have accumulated to suggest that insulin has effects on the brain, including a role in regulating brain glucose uptake and metabolism (41–43). Indeed, some effects associated with hyperglycemia are more likely caused by low insulin levels than by the hyperglycemia per se. In one study, diabetic rats were shown to have increased infarct volumes after ischemia/reperfusion injury compared with control

rats (44). Differences between the groups were eliminated by insulin treatment; however, treatment with TDZD-8 (a selective inhibitor of glycogen synthase kinase-β) to replicate one important pharmacological effect of insulin resulted in almost identical benefits despite persistence of hyperglycemia. Similarly, another study demonstrated reduced ADC values in diabetic rats (45). These values were normalized with insulin treatment, but treatment with IGF-1, resulting in insulin receptor activation, was found to have similar effects on ADC despite persistence of hyperglycemia.

Recent data support a neuroprotective role for insulin and suggest that lack of insulin in the brain, or absence of insulin effect, might cause or augment cerebral injury (46,47). Insulin-mediated signaling pathways have been hypothesized to be involved in regulation of neuronal survival, synaptic plasticity, learning, and memory function (46–48). Impairment of insulin receptor signaling in the brain has been proposed to contribute to age-related cognitive declines and has been suggested to play a role in several neurodegenerative disorders (46–49). Some investigators have hypothesized that insulin might exert neuroprotective effects under pathological conditions via stimulation of glucose metabolism resulting in increased brain levels of high-energy phosphates (47,50). Our results are of particular interest in this regard, as both low-insulin states evaluated in our study resulted in reductions in brain high-energy phosphates. In addition, insulin has been shown to enhance vasodilation and blood flow (24). Again, low insulin levels in both conditions in our study might be one possible explanation for the observed reductions in CBF.

The current study has some limitations. The level of ketosis achieved in the ketotic rats was lower than typically observed in children with DKA. Although greater ketosis could have been achieved with an intravenous ketone infusion, the fluid volume required for this infusion would cause changes in circulatory volume and therefore confounding effects on measures of CBF. In addition, higher ketone concentrations could result in metabolic acidosis with compensatory hypocapnia causing alterations in CBF. We therefore opted to evaluate more moderate ketosis and to use dietary manipulations to avoid altering circulatory volume. It is possible that the effects of ketosis might have been greater if higher concentrations of ketone bodies could have been achieved. In addition, several rats in the hyperglycemic group had mild metabolic acidosis, likely reflecting renal tubular acidosis resulting from nephrotoxic effects of streptozotocin treatment (11). We did not, however, detect any significant differences in magnetic resonance measures in hyperglycemic rats with or without RTA, and the degree of acidosis in all rats was mild and unlikely to cause any substantial physiological alterations.

In summary, our results suggest that hyperglycemia and ketosis both result in declines in CBF, reductions in cerebral high-energy phosphate concentrations, and brain cell swelling. The reductions in CBF resulting from hyperglycemia and/or ketosis help to explain the occurrence of cerebral hypoperfusion during DKA that appears to be greater than would be expected to result from hypocapnia and circulatory volume depletion alone. Furthermore, the apparently adverse effects of these conditions on cerebral metabolism might cause the brain to be more vulnerable to injury during modest hypoperfusion associated with DKA. Finally, the similarity in cerebral effects of hyperglycemia and ketosis raises the intriguing possibility that low insulin concentrations might be a predicating factor common to
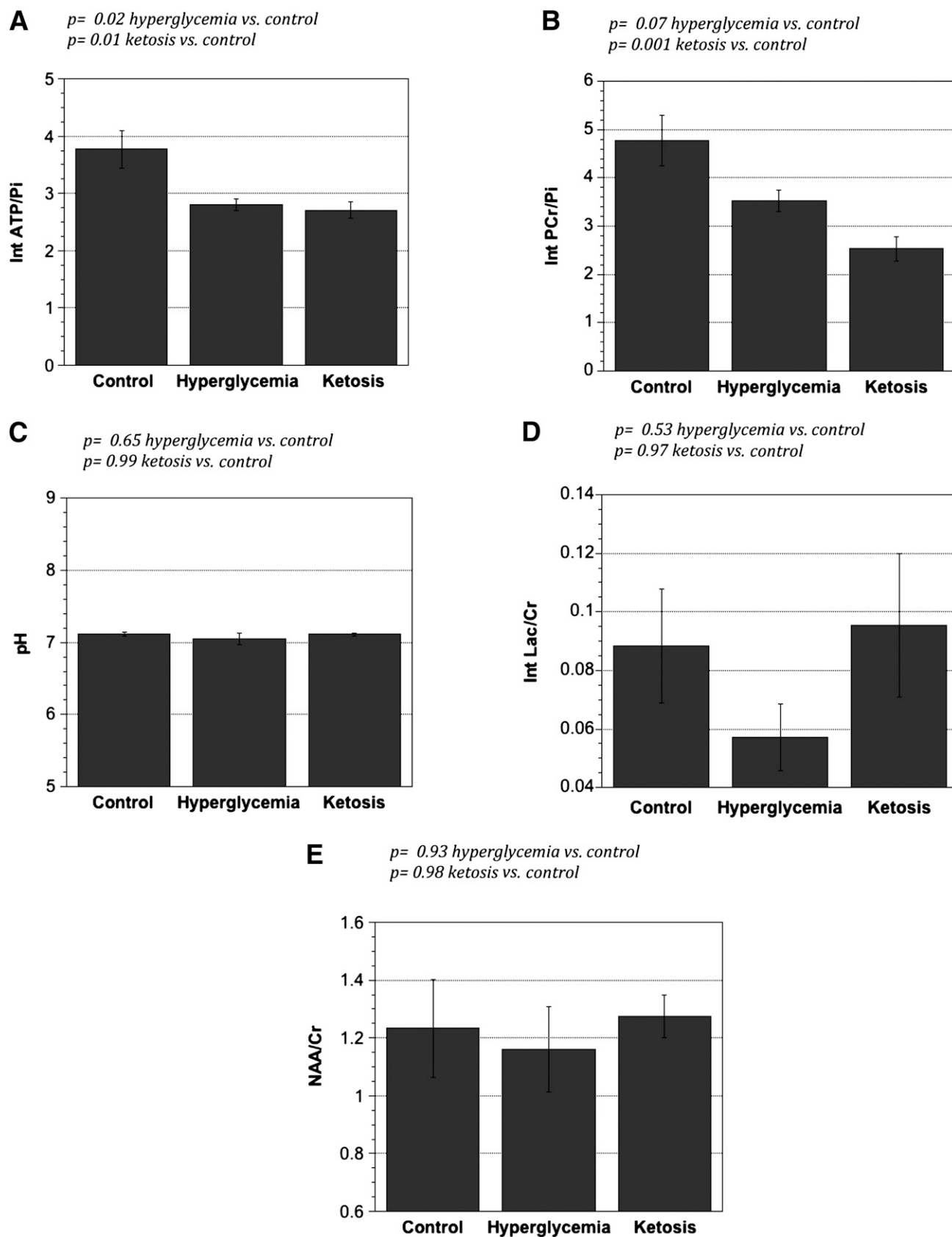
FIG. 2. Cerebral metabolites in hyperglycemic rats and ketotic rats in comparison with control rats measured using proton and phosphorus MRS (means ± SE; *n* = 7 for all groups). *A*: PCr-to-Pi ratio. *B*: ATP-to-Pi ratio. *C*: Intracellular (Int) pH. *D*: Lactate (Lac)-to-Cr ratio. *E*: NAA-to-Cr ratio.

both protocols or conditions. This hypothesis will require further investigation in future studies.

REFERENCES

1. Edge JA, Hawkins MM, Winter DL, Dunger DB. The risk and outcome of cerebral oedema developing during diabetic ketoacidosis. Arch Dis Child 2001;85:16–22
2. Glaser NS, Wootton-Gorges SL, Marcin JP, et al. Mechanism of cerebral edema in children with diabetic ketoacidosis. J Pediatr 2004;145:164–171
3. Wooton-Gorges S, Buonocore M, Caltagirone R, Kuppermann N, Glaser N. Progressive decrease in N-acetylaspartate/creatine ratio in a teenager with type 1 diabetes and repeated episodes of ketoacidosis without clinically apparent cerebral edema: evidence for permanent brain injury. AJNR Am J Neuroradiol 2010;31:780–781
4. Ghetti S, Lee J, Holtpatrick C, DeMaster D, Glaser N. Diabetic ketoacidosis and memory impairment in children with Type 1 diabetes. J Pediatr 2009;156:109–114
5. Glaser N, Yuen N, Anderson SE, Tancredi DJ, O'Donnell ME. Cerebral metabolic alterations in rats with diabetic ketoacidosis: effects of treatment with insulin and intravenous fluids and effects of bumetanide. Diabetes 2010;59:702–709
6. Yuen N, Anderson SE, Glaser N, Tancredi DJ, O'Donnell ME. Cerebral blood flow and cerebral edema in rats with diabetic ketoacidosis. Diabetes 2008;57:2588–2594
7. Lam TI, Anderson SE, Glaser N, O'Donnell ME. Bumetanide reduces cerebral edema formation in rats with diabetic ketoacidosis. Diabetes 2005;54:510–516
8. O'Donnell ME, Lam TI, Tran L, Anderson SE. The role of the blood-brain barrier Na-K-2Cl cotransporter in stroke. Adv Exp Med Biol 2004;559:67–75
9. Anderson SA, Carr LJ, Schierling TD, Kost GJ. Are age-related differences in response to myocardial ischemia and cardioplegia pH dependent? Biol Neonate 1994;65:25–35
10. Wootton-Gorges SL, Buonocore MH, Kuppermann N, et al. Detection of cerebral beta-hydroxy butyrate, acetoacetate, and lactate on proton MR spectroscopy in children with diabetic ketoacidosis. AJNR Am J Neuroradiol 2005;26:1286–1291
11. Fennell JS, Falls WF Jr. Streptozotocin nephrotoxicity: studies on the defect in renal tubular acidification. Clin Nephrol 1981;15:97–101
12. Taubin H, Matz R. Cerebral edema, diabetes insipidus, and sudden death during the treatment of diabetic ketoacidosis. Diabetes 1968;17:108–109
13. Young E, Bradley RF. Cerebral edema with irreversible coma in severe diabetic ketoacidosis. N Engl J Med 1967;276:665–669
14. Kucharczyk J, Moseley M, Kurhanewicz J, Norman D. MRS of ischemic/hypoxic brain disease. Invest Radiol 1989;24:951–954
15. Auld KL, Ashwal S, Holshouser BA, et al. Proton magnetic resonance spectroscopy in children with acute central nervous system injury. Pediatr Neurol 1995;12:323–334
16. Alvarez-Sabín J, Molina CA, Ribó M, et al. Impact of admission hyperglycemia on stroke outcome after thrombolysis: risk stratification in relation to time to reperfusion. Stroke 2004;35:2493–2498
17. Ennis SR, Keep RF. Effect of sustained-mild and transient-severe hyperglycemia on ischemia-induced blood-brain barrier opening. J Cereb Blood Flow Metab 2007;27:1573–1582
18. Huang NC, Wei J, Quast MJ. A comparison of the early development of ischemic brain damage in normoglycemic and hyperglycemic rats using magnetic resonance imaging. Exp Brain Res 1996;109:33–42
19. Parsons MW, Barber PA, Desmond PM, et al. Acute hyperglycemia adversely affects stroke outcome: a magnetic resonance imaging and spectroscopy study. Ann Neurol 2002;52:20–28
20. Ribo M, Molina CA, Delgado P, et al. Hyperglycemia during ischemia rapidly accelerates brain damage in stroke patients treated with tPA. J Cereb Blood Flow Metab 2007;27:1616–1622
21. Li PA, Shuaib A, Miyashita H, He QP, Siesjö BK, Warner DS. Hyperglycemia enhances extracellular glutamate accumulation in rats subjected to forebrain ischemia. Stroke 2000;31:183–192
22. Lin B, Ginsberg MD, Busto R, Li L. Hyperglycemia triggers massive neutrophil deposition in brain following transient ischemia in rats. Neurosci Lett 2000;278:1–4
23. Zygun DA, Steiner LA, Johnston AJ, et al. Hyperglycemia and brain tissue pH after traumatic brain injury. Neurosurgery 2004;55:877–881; discussion 882
24. Potenza MA, Gagliardi S, Nacci C, Carratu' MR, Montagnani M. Endothelial dysfunction in diabetes: from mechanisms to therapeutic targets. Curr Med Chem 2009;16:94–112
25. Evan-Wong LA, Davidson RJ, Stowers JM. Alterations in erythrocytes in hyperosmolar diabetic decompensation: a pathophysiological basis for impaired blood flow and for an improved design of fluid therapy. Diabetologia 1985;28:739–742
26. Sevick EM, Jain RK. Effect of red blood cell rigidity on tumor blood flow: increase in viscous resistance during hyperglycemia. Cancer Res 1991;51:2727–2730
27. Duckrow RB, Beard DC, Brennan RW. Regional cerebral blood flow decreases during chronic and acute hyperglycemia. Stroke 1987;18:52–58
28. Capes SE, Hunt D, Malmberg K, Pathak P, Gerstein HC. Stress hyperglycemia and prognosis of stroke in nondiabetic and diabetic patients: a systematic overview. Stroke 2001;32:2426–2432
29. Poppe AY, Majumdar SR, Jeerakathil T, Ghali W, Buchan AM, Hill MD; Canadian Alteplase for Stroke Effectiveness Study Investigators. Admission hyperglycemia predicts a worse outcome in stroke patients treated with intravenous thrombolysis. Diabetes Care 2009;32:617–622
30. Wang Y, Lim LL, Levi C, Heller RF, Fisher J. Influence of hyperglycemia on stroke mortality. J Stroke Cerebrovasc Dis 2001;10:11–18
31. Biessels GJ, Kamal A, Urban IJ, Spruijt BM, Erkelens DW, Gispen WH. Water maze learning and hippocampal synaptic plasticity in streptozotocin-diabetic rats: effects of insulin treatment. Brain Res 1998;800:125–135
32. Malone JI, Hanna S, Saporta S, et al. Hyperglycemia not hypoglycemia alters neuronal dendrites and impairs spatial memory. Pediatr Diabetes 2008;9:531–539
33. Isales C, Min L, Hoffman W. Acetoacetate and B-hydroxybutyrate differentially regulate endothelin-1 and vascular endothelial growth factor in mouse brain microvascular endothelial cells. J Diab Comp 1999;13:91–97
34. Jain SK, McVie R, Bocchini JA Jr. Hyperketonemia (ketosis), oxidative stress and type 1 diabetes. Pathophysiology 2006;13:163–170
35. Appelberg KS, Hovda DA, Prins ML. The effects of a ketogenic diet on behavioral outcome after controlled cortical impact injury in the juvenile and adult rat. J Neurotrauma 2009;26:497–506
36. Prins ML. Cerebral metabolic adaptation and ketone metabolism after brain injury. J Cereb Blood Flow Metab 2008;28:1–16
37. Puchowicz MA, Zechel JL, Valerio J, et al. Neuroprotection in diet-induced ketotic rat brain after focal ischemia. J Cereb Blood Flow Metab 2008;28:1907–1916
38. Wing RR, Vazquez JA, Ryan CM. Cognitive effects of ketogenic weight-reducing diets. Int J Obes Relat Metab Disord 1995;19:811–816

39. Zhao Q, Stafstrom CE, Fu DD, Hu Y, Holmes GL. Detrimental effects of the ketogenic diet on cognitive function in rats. Pediatr Res 2004;55:498–506

40. Linde R, Hasselbalch SG, Topp S, Paulson OB, Madsen PL. Global cerebral blood flow and metabolism during acute hyperketonemia in the awake and anesthetized rat. J Cereb Blood Flow Metab 2006;26:170–180

41. Bingham E, Hopkins D, Smith D, Pernet A, Hallett W, Reed L, et al. The role of insulin in human brain glucose metabolism: an 18fluoro-deoxyglucose positron emission tomography study. Diabetes 2002;51:3384–3390

42. Hoyer S, Henneberg N, Knapp S, Lannert H, Martin E. Brain glucose metabolism is controlled by amplification and desensitization of the neuronal insulin receptor. Ann N Y Acad Sci 1996;777:374–379

43. Doyle P, Cusin I, Rohner-Jeanrenaud F, Jeanrenaud B. Four-day hyperinsulinemia in euglycemic conditions alters local cerebral glucose utilization in specific brain nuclei of freely moving rats. Brain Res 1995;684:47–55

44. Collino M, Aragno M, Castiglia S, et al. Insulin reduces cerebral ischemia/reperfusion injury in the hippocampus of diabetic rats: a role for glycogen synthase kinase-3beta. Diabetes 2009;58:235–242

45. Haraldseth O, Jones RA, Skottner A. A quantitative in-vivo MR imaging study of brain dehydration in diabetic rats and rats treated with peptide hormones. Magn Reson Imaging 1997;15:203–210

46. Wickelgren I. Tracking insulin to the mind. Science 1998;280:517–519

47. Cardoso S, Correia S, Santos RX, et al. Insulin is a two-edged knife on the brain. J Alzheimers Dis 2009;18:483–507

48. Schulingkamp RJ, Pagano TC, Hung D, Raffa RB. Insulin receptors and insulin action in the brain: review and clinical implications. Neurosci Biobehav Rev 2000;24:855–872

49. Salkovic-Petrisic M, Osmanovic J, Grünblatt E, Riederer P, Hoyer S. Modeling sporadic Alzheimer's disease: the insulin resistant brain state generates multiple long-term morphobiological abnormalities including hyperphosphorylated tau protein and amyloid-beta. J Alzheimers Dis 2009;18:729–750

50. Duarte AI, Proença T, Oliveira CR, Santos MS, Rego AC. Insulin restores metabolic function in cultured cortical neurons subjected to oxidative stress. Diabetes 2006;55:2863–2870